The N-Terminus of Apolipoprotein A-V Adopts a Helix Bundle Molecular Architecture †

ARTICLE *in* BIOCHEMISTRY · AUGUST 2008

Impact Factor: 3.02 · DOI: 10.1021/bi800515c · Source: PubMed

Published in final edited form as:
Biochemistry. 2008 August 19; 47(33): 8768–8774. doi:10.1021/bi800515c.

The N-Terminus of Apolipoprotein A-V Adopts a Helix Bundle Molecular Architecture†

Kasuen Wong[‡,§], **Jennifer A. Beckstead**[‡], **Dustin Lee**[‡], **Paul M. M. Weers**[‖], **Emmanuel Guigard**[⊥], **Cyril M. Kay**[⊥], and **Robert O. Ryan**[*,‡,§]

[‡]Center for Prevention of Obesity, Diabetes and Cardiovascular Disease, Children's Hospital Oakland Research Institute, 5700 Martin Luther King Jr. Way, Oakland, California 94609

[§]Department of Nutritional Sciences and Toxicology, University of California, Berkeley, California 94720

[‖]Department of Chemistry and Biochemistry, California State University Long Beach, 1250 Bellflower Boulevard, Long Beach, California 90840

[⊥]Department of Biochemistry, University of Alberta, Edmonton, Alberta, T6G 2S2 Canada

Abstract

Previous studies of recombinant full-length human apolipoprotein A-V (apoA-V) provided evidence of the presence of two independently folded structural domains. Computer-assisted sequence analysis and limited proteolysis studies identified an N-terminal fragment as a candidate for one of the domains. C-Terminal truncation variants in this size range, apoA-V(1–146) and apoA-V(1–169), were expressed in *Escherichia coli* and isolated. Unlike full-length apoA-V or apoA-V(1–169), apoA-V(1–146) was soluble in neutral-pH buffer in the absence of lipid. Sedimentation equilibrium analysis yielded a weight-average molecular weight of 18811, indicating apoA-V(1–146) exists as a monomer in solution. Guanidine HCl denaturation experiments at pH 3.0 yielded a one-step native to unfolded transition that corresponds directly with the more stable component of the two-stage denaturation profile exhibited by full-length apoA-V. On the other hand, denaturation experiments conducted at pH 7.0 revealed a less stable structure. In a manner similar to that of known helix bundle apolipoproteins, apoA-V(1–146) induced a relatively small enhancement in 8-anilino-1-naphthalenesulfonic acid fluorescence intensity. Quenching studies with single-Trp apoA-V(1–146) variants revealed that a unique site predicted to reside on the nonpolar face of an amphipathic α-helix was protected from quenching by KI. Taken together, the data suggest the 146 N-terminal residues of human apoA-V adopt a helix bundle molecular architecture in the absence of lipid and, thus, likely exist as an independently folded structural domain within the context of the intact protein.

Hypertriglyceridemia (HTG)[1] is strongly and positively correlated with susceptibility to atherosclerosis (1). Furthermore, HTG is a risk factor for development of the metabolic syndrome and the accompanying insulin resistance, hypertension, obesity, and inflammation. On this basis, there is considerable interest in understanding factors that regulate plasma triglyceride (TG) levels. The discovery of a new apolipoprotein in 2001, termed apolipoprotein

†This work was supported by grants from the National Institutes of Health to R.O.R. (HL 073061) and P.M.M.W. (HL 077135) and the Alberta Cancer Board to C.M.K.

*To whom correspondence should be addressed. rryan@chori.org. Telephone: (510) 450-7645. Fax: (510) 450-7910.

[1]Abbreviations: apo, apolipoprotein; HTG, hypertriglyceridemia; TG, triglyceride; HDL, high-density lipoprotein; VLDL, very low-density lipoprotein; CFE, carbon-filled Epon; CD, circular dichroism; ANS, 8-anilino-1-naphthalenesulfonic acid; SDS, sodium dodecyl sulfate; PAGE, polyacrylamide gel electrophoresis; NT, amino-terminal.

(apo) A-V, has sparked an intensive research effort (2,3). The impact of apoA-V on plasma TG levels is vividly illustrated by the seminal report of Pennacchio et al. (4). Using genetically modified mice, these authors showed that plasma TG concentrations in human *APOA5* transgenic mice were 3-fold lower than those of control littermates. At the same time, apoA-V gene-disrupted mice exhibited a 4-fold increase in plasma TG concentration.

Human apoA-V is synthesized in the liver as a 366-amino acid preprotein. Following cleavage of a 23-amino acid signal peptide, mature apoA-V, consisting of 343 residues, can be detected in plasma (5). Comparative sequence analysis indicates apoA-V is a member of the class of exchangeable apolipoproteins and predicts a hydrophobic protein with a significant amount of α-helical secondary structure (6). This prediction has been confirmed by far-UV circular dichroism spectroscopy analysis (7). A distinguishing feature of recombinant lipid-free apoA-V is poor solubility in neutral-pH buffer (8). Characterization studies of lipid-free apoA-V revealed strong lipid binding activity (6). Consistent with this, apoA-V is found exclusively associated with lipoproteins in the plasma compartment. In mice, apoA-V is predominantly associated with HDL (9), while in humans, it is found in the VLDL and HDL fractions (10). Evidence suggests that apoA-V can exchange between VLDL and HDL, possibly as a function of plasma lipoprotein homeostasis (9).

In 2005, Marçais et al. reported the presence of a mutant form of apoA-V in a family with HTG (11). The mutation introduces a premature stop codon, resulting in a truncated apoA-V variant that is recovered in the lipoprotein-deficient fraction of plasma. These data suggest the C-terminal portion of apoA-V is a determinant of its lipoprotein binding ability. Subsequent studies revealed the C-terminus contributes to the lipid binding activity of apoA-V (7). It was reported that deletion of the 51 C-terminal amino acids from apoA-V resulted in a variant protein that exhibited lower lipid binding activity yet still possessed two independently folded structural domains. In this study, we sought to define the boundary between these domains and to characterize the N-terminal domain in isolation. The results obtained reveal that lipid-free apoA-V(1–146) adopts a relatively stable, monomeric, asymmetric tertiary fold that is consistent with an amphipathic α-helix bundle.

MATERIALS AND METHODS

Site-Directed Mutagenesis and Overexpression of Recombinant Proteins

Recombinant human apoA-V and C-terminal truncation variants were produced in *Escherichia coli* and isolated as described previously (8). The apoE NT domain was prepared as described by Fisher et al. (12), and apolipophorin III was prepared as described by Ryan et al. (13). Site-directed mutagenesis was performed with the QuikChange II XL site-directed mutagenesis kit (Stratagene). Primers were designed to introduce a premature stop codon or to substitute Trp5 with Phe and Trp97 with Phe or substitute Leu73 of null apoA-V(1–146) with Trp. In all cases, introduction of the desired mutations was verified by DNA sequencing.

Limited Proteolysis

Aliquots of full-length apoA-V (0.1 mg/mL) in 50 mM sodium citrate (pH 3.0) and 150 mM NaCl were incubated with 0.1 μg/mL porcine gastric pepsin (Sigma) at 22 °C for up to 2 h. The reaction was stopped by addition of SDS-PAGE sample treatment buffer and the fragmentation pattern assessed by SDS gel electrophoresis on a Tricine, 10 to 20% acrylamide slab run at a constant 125 V for 1.5 h and stained with Gel Code Blue (Pierce Chemical Co.). Where indicated, separated protein fragments were electrophoretically transferred to a PVDF membrane and then subjected to N-terminal sequencing analysis (Molecular Structure Facility, University of California, Davis, CA).

Analytical Procedures

Protein concentrations were determined with the bicinchoninic acid assay (Pierce Chemical Co.) using bovine serum albumin as the standard.

Analytical Ultracentrifugation

Sedimentation equilibrium experiments were conducted at 20 °C in a Beckman XL-I analytical ultracentrifuge using interference optics, as described by Laue and Stafford (14). Aliquots (110 μL) of the sample solution were loaded into six-sector CFE sample cells, allowing three concentrations to be run simultaneously. Runs were performed at three different speeds, and each speed was maintained until there was no significant difference in $r^2/2$ versus absorbance scans taken 2 h apart to ensure that equilibrium was achieved. Sedimentation equilibrium data were evaluated using the NONLIN program, which employs the nonlinear least-squares curve fitting algorithm described by Johnson et al. (15). The protein's partial specific volume and the solvent density were estimated using Sednterp (16). Sedimentation velocity experiments were conducted at 40000 rpm and 20 °C using absorbance optics. Runs were performed at loading concentrations of 0.55 and 0.24 mg/mL. Up to 260 scans were performed during the run. A sedimentation coefficient value was obtained by analyzing 10 sets of data selected between the 160th and 205th scans using Svedberg. From the amino acid composition, a hydration value of 0.44 was obtained, assuming that all charged groups are exposed.

Circular Dichroism Spectroscopy

Circular dichroism (CD) measurements were performed on an AVIV 410 spectrophotometer or a Jasco 810 spectropolarimeter. Far-UV CD scans were recorded between 185 and 260 nm in 20 mM sodium phosphate (pH 7.4) using a protein concentration of 0.5 mg/mL determined by the absorbance at 280 nm. The α-helical content was calculated with the self-consistent method using Dicroprot, version 2.6 (17). For guanidine HCl denaturation studies, protein samples were dissolved in 50 mM citrate (pH 3.0) or 20 mM sodium phosphate (pH 7.4). ApoA-V samples (0.2 mg/mL) were incubated overnight at a given denaturant concentration to attain equilibrium, and ellipticity was measured at 222 nm.

Fluorescence Spectroscopy

Fluorescence spectra were recorded on a Horiba Jobin Yvon FluoroMax-4 luminescence spectrometer. Protein (100 μg/mL) was dissolved in either 50 mM citrate (pH 3.0) with 150 mM NaCl or 20 mM sodium phosphate (pH 7.4) with 150 mM NaCl. Samples were excited at 295 nm, and emission was collected from 300 to 450 nm (2.0 nm slit width). Spectra of 8-anilino-1-naphthalenesulfonic acid (ANS) solutions (250 mM) were obtained in pH 7.4 buffer alone and in the presence of specified proteins at 50 μg/mL. Samples were excited at 395 nm with emission monitored from 400 to 600 nm (2.0 nm slit width). Since ANS fluorescence in buffer is negligible (18), spectra were recorded in the presence of a minimum 100-fold excess of ANS with respect to protein (molar ratio). For KI quenching studies, protein samples were excited at 295 nm and emission was monitored at their λ_{max} values. The solution of KI contained 1 mM sodium thiosulfate to prevent formation of free iodine, and all readings were corrected for dilution. The data were analyzed using the Stern-Volmer equation: $F_0/F = 1 + K_{SV}[Q]$, where F_0 and F represent the emission intensity maximum in the absence and presence of quencher, respectively. The collisional quenching constant (K_{SV}) was determined from the initial slope of plots of F_0/F versus [Q].

RESULTS

Limited Proteolysis of Full-Length ApoA-V

On the basis of similarities with other members of the exchangeable apolipoprotein family (19,20), we hypothesized that the N-terminus of apoA-V may exist in solution as an independently folded, amphipathic α-helix bundle. In the case of another two-domain apolipoprotein, apoE, limited proteolysis yielded two major fragments (21,22) that were shown to exist as independently folded structural domains (23,24). Due to the insolubility of lipid-free full-length apoA-V at neutral pH, proteolytic digestion experiments were conducted at pH 3.0 using pepsin. Isolated recombinant apoA-V was incubated with pepsin (1000:1, w/w) as a function of time, followed by SDS-PAGE analysis of the digestion products (Figure 1). The data showed that, as intact apoA-V was rapidly degraded, two prominent fragments, one of ~22 kDa and the other of ~18 kDa, were generated. At longer time points, or higher protease concentrations, complete degradation of apoA-V occurred (data not shown). On the basis of the apparent protection of the 18 and 22 kDa fragments from limited proteolysis, these fragments were subjected to further characterization. Electrospray ionization mass spectrometry analysis yielded molecular mass values of 18721.2 and 22198.9 Da. N-Terminal sequencing of the cleavage products revealed the first 7–10 amino acid residues of the 18 kDa band correspond to V-S-G-I-G-R-H-V-Q-E-L, while that for the 22 kDa band was M-H-H-H-H-H-H. Since recombinant apoA-V employed in the proteolysis studies possessed an N-terminal His-tag extension, we conclude that the larger cleavage product corresponds to the N-terminal portion of apoA-V (residues 1–175). The identity of the smaller 18 kDa band corresponds to apoA-V residues 176–343, presumably encompassing the C-terminal structural domain of apoA-V.

In Silico Analysis of the ApoA-V N-Terminal Domain

Evaluation of the N-terminal sequence of apoA-V (residues 1–175) with Coils (25) predicts that residues Ala31-Arg52, Val67-Gln85, and Asp112-Asp134 adopt α-helix secondary structure. Given that a hallmark feature of the class of exchangeable apolipoproteins is the presence of amphipathic α-helices approximately 22 amino acids in length, we sought to assess if these predicted helices would display amphipathic character [i.e., possess distinct nonpolar and polar faces with positively charged amino acids located at the interface between the polar and nonpolar faces, while negatively charged residues reside at the apex of the polar face (26)]. An Edmundson wheel (27) projection of the sequence from Gly68 to Gln85 reveals these characteristic features (Figure 2) consistent with earlier hydropathy analysis (6). Furthermore, similar to other members of the class of exchangeable apolipoproteins, two of the three α-helix segments predicted with Coils are punctuated by proline residues (Figure 3).

Isolation and Characterization of ApoA-V(1–146)

In an effort to study the N-terminal fragment of apoA-V in greater detail, two truncation variants, apoA-V(1–169) and apoA-V(1–146), were expressed in *E. coli*, isolated, and characterized (Figure 4). ApoA-V(1–292) was previously characterized and found to possess two structural domains (7). Unlike full-length apoA-V, apoA-V(1–292), or apoA-V(1–169), apoA-V(1–146) was soluble in aqueous buffer at neutral pH. Furthermore, limited proteolysis experiments with apoA-V(1–146) revealed resistance to further degradation. Given the favorable solubility properties of this variant and the apparent similarity of this truncated apoA-V variant to one of the protease resistant fragments generated upon pepsin treatment of full-length apoA-V, characterization studies of apoA-V(1–146) were performed.

Hydrodynamic Properties

The hydrodynamic properties of apoA-V(1–146) were investigated by sedimentation equilibrium analyses performed at pH 7.0 (Table 1). The initial centrifugation speed was set at 22000 rpm, and equilibrium was reached after 18 h. Data were collected at 22000, 24000, and 26000 rpm. The apparent average molecular mass of apoA-V(1–146) was 18811 Da, a value that corresponds well with the calculated molecular mass of this protein (18795 Da). These data indicate that, unlike full-length apoA-V (8), apoA-V(1–146) exists in solution as a monomer. To evaluate the shape of apoA-V(1–146) in solution, sedimentation velocity experiments were conducted. Using Svedberg, the data were fit to a single-species model yielding a sedimentation coefficient of ~1.8. Sednterp was then used to calculate an axial ratio value. Using a prolate model and a hydration expansion of 17.1%, an axial ratio (*a*/*b*) of 7 was obtained.

CD Spectroscopy and Stability Studies

Far-UV CD spectroscopy of apoA-V(1–146) at pH 7.4 yielded a spectrum with minima at 208 and 222 nm. Deconvolution of the spectra yielded an α-helix secondary structure content of 40.4%, consistent with predictions from Coils analysis. To assess the stability properties of apoA-V(1–146) in solution, the effects of guanidine HCl concentration on ellipticity values at 222 nm were determined (Figure 5). At pH 3.0 (pH at which comparisons with data on full-length apoA-V can be made), as the concentration of denaturant increased form 0 to 4 M, apoA-V(1–146) unfolded in a single transition, with a midpoint at 2.0 M guanidine HCl. At pH 7.4, although apoA-V(1–146) still undergoes a one-step native → unfolded transition, the transition midpoint is shifted to 0.9 M guanidine HCl, a value similar to that reported for apoA-I (28).

Fluorescent Dye Binding Studies

ANS, a hydrophobic fluorescent dye, binds to exposed hydrophobic surfaces in proteins (18). In the absence of protein, ANS has a very low quantum yield with an emission wavelength maximum of ~520 nm (excitation at 395 nm). Albumin, a serum lipid transport protein known to possess exposed hydrophobic lipid binding sites, induced a significant enhancement in ANS fluorescence intensity as well as a blue shift in the wave-length of maximum fluorescence emission at pH 7.4 (Figure 6). By contrast, known helix bundle apolipoproteins, including apoE3 NT (29) and apolipophorin III (30), had a weaker effect on ANS fluorescence intensity. In a similar manner, apoA-V(1–146) induced a relatively small enhancement in ANS fluorescence intensity, consistent with sequestration of hydrophobic sites in this protein from the aqueous milieu.

Tryptophan Fluorescence Emission of ApoA-V(1–146) Variants

ApoA-V(1–146) has two naturally occurring Trp residues, located at positions 5 and 97. Fluorescence emission (excitation at 295 nm) spectra of wild-type apoA-V(1–146) gave rise to a λ_{max} of 350 nm (Table 2). To determine the individual contribution of the two Trp residues in this protein, single-Trp variant apoA-V(1–146) forms were generated. To test the hypothesis that apoA-V(1–146) adopts a helix bundle conformation in solution, a single Trp was also introduced into Trp-null apoA-V(1–146) by replacing Leu73 with Trp. On the basis of predictions, this sequence position should reside on the nonpolar face of an amphipathic α-helix (see Figure 2). At neutral pH, the λ_{max} of each of the three single-Trp variants was 349 nm. In contrast, when Trp fluorescence emission was monitored at pH 3.0, both the Trp73 and Trp97 variants show a blue shift in λ_{max} to 338 and 341 nm, respectively (Table 2).

Fluorescence Quenching

To obtain additional information about the local environments of Trp5, Trp97, and Trp73 in single-Trp apoA-V(1–146) variants, fluorescence quenching studies were performed with

potassium iodide (KI) as the quenching agent. Stern-Volmer plots for each single-Trp variant were linear (Figure 7), and K_{SV} constants were obtained from the slope of the plots. The values were 3.2 M^{-1} for the Trp5 variant, 2.2 M^{-1} for the Trp97 variant, and 1.8 M^{-1} for the Trp73 variant.

DISCUSSION

The amphipathic α-helix bundle is a common structural motif among exchangeable apolipoproteins in their lipid-free state. X-ray crystallography studies of the apoE NT domain (29), apolipophorin III (31), and apoA-I (20) reveal elongated up-and-down bundles of four or five amphipathic α-helices. In every case, the helices orient such that their hydrophobic faces are directed toward the bundle interior. At the same time, hydrophilic moieties are directed to the solvent, conferring aqueous solubility to these proteins (32). In this study, the data are consistent with the presence of at least three distinct α-helices in apoA-V(1–146). Whereas the three-helix bundle motif exists among helix bundle proteins in general (33–35), no three-helix bundle motifs have been reported for apolipoproteins. Evidence of the presence of only three helix segments in apoA-V(1–146) is based upon predictions from Coils analysis. However, caution must be exercised in this case since a similar analysis of human apoE3 N-terminal domain primary structure predicts residues 1–183 also possess three distinct helix segments. Whereas Coils analysis faithfully predicts the boundaries for three of the four known helices [on the basis of X-ray crystallography (29)] to exist in the apoE NT domain, helix 1 was not identified with this program. On the basis of this, it is conceivable that apoA-V(1–146) may possess a fourth helix segment that was simply not predicted by Coils analysis. Given the location of the three identified helix segments, a fourth helix, if present, could be located at the extreme N-terminus of this truncated apoA-V or between proline residues 86 and 108, consistent with fluorescence quenching data of Trp97. In fact, apoA-V(1–146) could conceivably contain five amphipathic helices, which has been shown with apolipophorin III (30,31). The actual tertiary organization of the apoA-V NT domain will require detailed high-resolution structure data from NMR spectroscopy and/or X-ray crystallography.

On the basis of structural studies and other evidence, hypotheses have been proposed to explain the lipid surface seeking behavior of helix bundle apolipoproteins. Thus, whereas hydrophobic helix–helix interactions contribute to stabilization of the bundle conformation, these interactions are replaced by helix–lipid interactions in a lipid-associated state. Such a transition, however, requires that the bundle undergo conformational “opening” to expose hydrophobic lipid binding sites in the protein interior (19,20,36). Several lines of evidence are consistent with this hypothesis, and in the case of the apoE NT domain, this transition plays a key role in manifestation of its low-density lipoprotein receptor recognition properties (37). Given the evidence that apoA-V(1–146) adopts a helix bundle motif, it is likely that a similar transition occurs upon association of lipid with this protein.

In certain helix bundle apolipoproteins, the helix bundle motif constitutes the sole structural element of the protein (30,31). In other cases, however, the helix bundle motif exists as a domain in the context of a larger protein. Thus, for example, apoE exists as a two-domain protein comprised of an N-terminal helix bundle and a C-terminal lipid binding domain (19). Likewise, the N-terminus of apoA-I adopts a helix bundle that is connected to a short C-terminal segment with high lipid binding affinity (20). Given the relatively large size of apoA-V and the results of guanidine HCl denaturation studies (7), it is evident that two independently folded structural domains are present. Furthermore, recent studies with another C-terminal truncation variant, apoA-V(1–292), provided evidence that the N-terminus comprises the more stable component of the two structural elements in apoA-V (7). In the case of apoE, the 165 N-terminal amino acids adopt a four-helix bundle conformation (38). From denaturation data, primary sequence analysis, and limited proteolysis, it may be concluded that the N-terminus of apoA-

V adopts a similar molecular architecture in the absence of lipid. Indeed, several lines of evidence indicate that the 146 N-terminal amino acids of apoA-V exist as a helix bundle. Evidence supporting this interpretation includes the solubility properties of apoA-V(1–146). Whereas full-length apoA-V and truncation variants longer than 146 residues are insoluble in neutral-pH buffer, this is not the case for apoA-V(1–146). In general, it is envisioned that solubility is conferred to helix bundle apolipoproteins because of their ability to sequester hydrophobic lipid binding sites in the bundle interior. Because of this, isolated helix bundle apolipoproteins often exist in solution in a monomeric state (24). In the case of apoA-V(1–146), sedimentation equilibrium experiments provide evidence that the protein exists in solution as a monomer, and consistent with other helix bundle apolipoproteins, sedimentation velocity experiments yielded an axial ratio value that is consistent with a highly asymmetric structure. Similar values have been reported for helix bundle apolipoproteins (39), and these findings are supported by high-resolution structure data (20,29–31).

An ability of helix bundle apolipoproteins to sequester their hydrophobic lipid binding sites in the bundle interior is generally manifest by a weaker ability to enhance the fluorescence signal of ANS relative to proteins known to have exposed hydrophobic sites (40). ApoA-V(1–146) behaved like apolipophorin III and the apoE3 NT domain, suggesting it too adopts a helix bundle structure. On the basis of Coils analysis, the Trp at position 5 is predicted to be solvent-exposed. Fluorescence quenching studies with KI at pH 7.4 show Trp5 is more susceptible to quenching, consistent with its location at the extreme N-terminus of the protein. On the other hand, Trp73 is anticipated to reside on the hydrophobic face of an amphipathic α-helix on the basis of Coils and Edmundson wheel analyses. The λ_{max} of Trp73 at 338 nm (at pH 3.0) suggests it resides in a more nonpolar environment under these conditions. KI quenching studies with apoA-V(1–146) Trp73 reveal the Trp at this position is relatively protected from this quencher, providing additional evidence of its proposed location within a helix bundle. KI quenching shows Trp97 to be more protected from the quencher than Trp5 but not more than Trp73. Thus, it is conceivable that the region encompassing Trp97 adopts amphipathic α-helix secondary structure. While Trp73 was the least susceptible to fluorescence quenching, it was not completely inaccessible, which along with the Trp fluorescence emission results and the denaturation studies at pH 7.4, implies that the apoA-V NT domain at neutral pH may adopt a “loosely” folded helix bundle under physiological conditions. Given the greater propensity of molten globule-like conformations in apolipoproteins to associate with lipid surfaces (41), this property may be relevant to the function of this structural element in apoA-V, possibly in concert with the C-terminal region of intact apoA-V.

At present, it is unknown if the NT domain of apoA-V alone is capable of manifesting biological effects seen with full-length apoA-V. On the basis of results of studies of a mutant and/or truncated form of apoA-V in human subjects that is associated with severe HTG (11), this segment of the protein alone may not be sufficient to manifest the biological effects seen with apoA-V in genetically engineered mice. Indeed, previous studies have suggested that residues in the region of residues 186–242 in apoA-V are responsible for the heparin binding ability of apoA-V (42) as well as its function as a ligand for members of the low-density lipoprotein receptor family (43) or recently identified gly-cosylphosphatidylinositol high-density lipoprotein binding protein 1 (44). Adenovirus-mediated gene transfer of apoA-V(1–146) into apoA-V gene-disrupted mice will permit this question to be addressed.

Acknowledgments

We thank Dr. David King and Dr. Susan Marqusee for mass spectrometry and access to the circular dichroism spectrometer, respectively.

REFERENCES

1. Yuan G, Al-Shali KZ, Hegele RA. Hypertrig-lyceridemia: Its etiology, effects and treatment. Can. Med. Assoc. J 2007;176:1113–1120. [PubMed: 17420495]
2. Jakel H, Nowak M, Helleboid-Chapman A, Fruchart-Najib J, Fruchart JC. Is apolipoprotein A5 a novel regulator of triglyceride-rich lipoproteins? Ann. Med 2006;38:2–10. [PubMed: 16448983]
3. Wong K, Ryan RO. Characterization of apolipo-protein A-V structure and mode of plasma triacylglycerol regulation. Curr. Opin. Lipidol 2007;18:319–324. [PubMed: 17495607]
4. Pennacchio LA, Olivier M, Hubacek JA, Cohen JC, Cox DR, Fruchart JC, Krauss RM, Rubin EM. An apolipoprotein influencing triglycerides in humans and mice revealed by comparative sequencing. Science 2001;294:169–173. [PubMed: 11588264]
5. Alborn WE, Johnson MG, Prince MJ, Konrad RJ. Definitive N-terminal protein sequence and further characterization of the novel apolipoprotein A5 in human serum. Clin. Chem 2006;52:514–517. [PubMed: 16510431]
6. Weinberg RB, Cook VR, Beckstead JA, Martin DD, Gallagher JW, Shelness GS, Ryan RO. Structure and interfacial properties of human apolipoprotein A-V. J. Biol. Chem 2003;278:34438–34444. [PubMed: 12810715]
7. Beckstead JA, Wong K, Gupta V, Wan CP, Cook VR, Weinberg RB, Weers PM, Ryan RO. The C terminus of apolipoprotein A-V modulates lipid-binding activity. J. Biol. Chem 2007;282:15484–15489. [PubMed: 17401142]
8. Beckstead JA, Oda MN, Martin DD, Forte TM, Bielicki JK, Berger T, Luty R, Kay CM, Ryan RO. Structure-function studies of human apolipoprotein A-V: A regulator of plasma lipid homeostasis. Biochemistry 2003;42:9416–9423. [PubMed: 12899628]
9. Nelbach L, Shu X, Konrad RJ, Ryan RO, Forte TM. Effect of apolipoprotein A-V on plasma triglyceride, lipoprotein size, and composition in genetically engineered mice. J. Lipid Res 2008;49:572–580. [PubMed: 18056685]
10. O'Brien PJ, Alborn WE, Sloan JH, Ulmer M, Boodhoo A, Knierman MD, Schultze AE, Konrad RJ. The novel apolipoprotein A5 is present in human serum, is associated with VLDL, HDL, and chylomicrons, and circulates at very low concentrations compared with other apolipoproteins. Clin. Chem 2005;51:351–359. [PubMed: 15528295]
11. Marcais C, Verges B, Charriere S, Pruneta V, Merlin M, Billon S, Perrot L, Drai J, Sassolas A, Pennacchio LA, Fruchart-Najib J, Fruchart JC, Durlach V, Moulin P. Apoa5 Q139X truncation predisposes to late-onset hyper-chylomicronemia due to lipoprotein lipase impairment. J. Clin. Invest 2005;115:2862–2869. [PubMed: 16200213]
12. Fisher CA, Wang J, Francis GA, Sykes BD, Kay CM, Ryan RO. Bacterial overexpression, isotope enrichment, and NMR analysis of the N-terminal domain of human apolipoprotein E. Biochem. Cell Biol 1997;75:45–53. [PubMed: 9192073]
13. Ryan RO, Schieve D, Wientzek M, Narayanaswami V, Oikawa K, Kay CM, Agellon LB. Bacterial expression and site-directed mutagenesis of a functional recombinant apolipoprotein. J. Lipid Res 1995;36:1066–1072. [PubMed: 7658154]
14. Laue TM, Stafford WF. Modern applications of analytical ultracentrifugation. Annu. Rev. Biophys. Biomol. Struct 1999;28:75–100. [PubMed: 10410796]
15. Johnson ML, Correia JJ, Yphantis DA, Halvorson HR. Analysis of data from the analytical ultracentrifuge by nonlinear least-squares techniques. Biophys. J 1981;36:575–588. [PubMed: 7326325]
16. Laue, TM.; Shah, BD.; Ridgeway, TM.; Pelletier, SL. Analytical Ultracentrifugation in Biochemistry and Polymer Science. Cambridge, U.K.: Royal Society of Chemistry; 1991.
17. Sreerama N, Woody RW. A self-consistent method for the analysis of protein secondary structure from circular dichroism. Anal. Biochem 1993;209:32–44. [PubMed: 8465960]
18. Stryer L. The interaction of a naphthalene dye with apomyoglobin and apohemoglobin. A fluorescent probe of non-polar binding sites. J. Mol. Biol 1965;13:482–495. [PubMed: 5867031]
19. Weisgraber KH. Apolipoprotein E: Structure-function relationships. Adv. Protein Chem 1994;45:249–302. [PubMed: 8154371]

20. Ajees AA, Anantharamaiah GM, Mishra VK, Hussain MM, Murthy HM. Crystal structure of human apolipoprotein A-I: Insights into its protective effect against cardiovascular diseases. Proc. Natl. Acad. Sci. U.S.A 2006;103:2126–2131. [PubMed: 16452169]
21. Bradley WA, Gilliam EB, Gotto AM Jr, Gianturco SH. Apolipoprotein-E degradation in human very low density lipoproteins by plasma protease(s): Chemical and biological consequences. Biochem. Biophys. Res. Commun 1982;109:1360–1367. [PubMed: 6301435]
22. Innerarity TL, Friedlander EJ, Rall SC Jr, Weisgraber KH, Mahley RW. The receptor-binding domain of human apolipoprotein E. Binding of apolipoprotein E fragments. J. Biol. Chem 1983;258:12341–12347. [PubMed: 6313652]
23. Wetterau JR, Aggerbeck LP, Rall SC Jr, Weisgraber KH. Human apolipoprotein E3 in aqueous solution. I. Evidence for two structural domains. J. Biol. Chem 1988;263:6240–6248. [PubMed: 3360781]
24. Aggerbeck LP, Wetterau JR, Weisgraber KH, Wu CS, Lindgren FT. Human apolipoprotein E3 in aqueous solution. II. Properties of the amino- and carboxyl-terminal domains. J. Biol. Chem 1988;263:6249–6258. [PubMed: 3360782]
25. Lupas A, Van Dyke M, Stock J. Predicting coiled coils from protein sequences. Science 1991;252:1162–1164.
26. Segrest JP, Jones MK, De Loof H, Brouillette CG, Venkatachalapathi YV, Anantharamaiah GM. The amphipathic helix in the exchangeable apolipoproteins: A review of secondary structure and function. J. Lipid Res 1992;33:141–166. [PubMed: 1569369]
27. Schiffer M, Edmundson AB. Use of helical wheels to represent the structures of proteins and to identify segments with helical potential. Biophys. J 1967;7:121–135. [PubMed: 6048867]
28. Reijngoud DJ, Phillips MC. Mechanism of dissociation of human apolipoprotein A-I from complexes with dimyristoylphosphatidylcholine as studied by guanidine hydrochloride denaturation. Biochemistry 1982;21:2969–2976. [PubMed: 6809042]
29. Wilson C, Wardell MR, Weisgraber KH, Mahley RW, Agard DA. Three-dimensional structure of the LDL receptor-binding domain of human apolipoprotein E. Science 1991;252:1817–1822. [PubMed: 2063194]
30. Wang J, Sykes BD, Ryan RO. Structural basis for the conformational adaptability of apolipophorin III, a helix-bundle exchangeable apolipoprotein. Proc. Natl. Acad. Sci. U.S.A 2002;99:1188–1193. [PubMed: 11818551]
31. Breiter DR, Kanost MR, Benning MM, Wesenberg G, Law JH, Wells MA, Rayment I, Holden HM. Molecular structure of an apolipoprotein determined at 2.5-Å resolution. Biochemistry 1991;30:603–608. [PubMed: 1988048]
32. Wang J, Narayanaswami V, Sykes BD, Ryan RO. Interhelical contacts are required for the helix bundle fold of apolipophorin III and its ability to interact with lipoproteins. Protein Sci 1998;7:336–341. [PubMed: 9521109]
33. Evans CL, Long JE, Gallagher TR, Hirst JD, Searle MS. Conformation and dynamics of the three-helix bundle UBA domain of p62 from experiment and simulation. Proteins 2008;71:227–240. [PubMed: 17932931]
34. Yang JS, Wallin S, Shakhnovich EI. Universality and diversity of folding mechanics for three-helix bundle proteins. Proc. Natl. Acad. Sci. U.S.A 2008;105:895–900. [PubMed: 18195374]
35. Worrall LJ, Walkinshaw MD. Crystal structure of the C-terminal three-helix bundle subdomain of *C. elegans* Hsp70. Biochem. Biophys. Res. Commun 2007;357:105–110. [PubMed: 17407764]
36. Narayanaswami V, Wang J, Schieve D, Kay CM, Ryan RO. A molecular trigger of lipid binding-induced opening of a helix bundle exchangeable apolipoprotein. Proc. Natl. Acad. Sci. U.S.A 1999;96:4366–4371. [PubMed: 10200268]
37. Raussens V, Fisher CA, Goormaghtigh E, Ryan RO, Ruysschaert JM. The low density lipoprotein receptor active conformation of apolipoprotein E. Helix organization in N-terminal domain-phospholipid disc particles. J. Biol. Chem 1998;273:25825–25830. [PubMed: 9748256]
38. Segelke BW, Forstner M, Knapp M, Trakhanov SD, Parkin S, Newhouse YM, Bellamy HD, Weisgraber KH, Rupp B. Conformational flexibility in the apolipoprotein E amino-terminal domain structure determined from three new crystal forms: Implications for lipid binding. Protein Sci 2000;9:886–897. [PubMed: 10850798]

39. Kiss RS, Kay CM, Ryan RO. Amphipathic αhelix bundle organization of lipid-free chicken apolipoprotein A-I. Biochemistry 1999;38:4327–4334. [PubMed: 10194351]

40. Weers PM, Narayanaswami V, Ryan RO. Modulation of the lipid binding properties of the N-terminal domain of human apolipoprotein E3. Eur. J. Biochem 2001;268:3728–3735. [PubMed: 11432739]

41. Soulages JL, Bendavid OJ. The lipid binding activity of the exchangeable apolipoprotein apolipophorin-III correlates with the formation of a partially folded conformation. Biochemistry 1998;37:10203–10210. [PubMed: 9665727]

42. Lookene A, Beckstead JA, Nilsson S, Olivecrona G, Ryan RO. Apolipoprotein A-V-heparin interactions: Implications for plasma lipoprotein metabolism. J. Biol. Chem 2005;280:25383–25387. [PubMed: 15878877]

43. Nilsson SK, Lookene A, Beckstead JA, Gliemann J, Ryan RO, Olivecrona G. Apolipoprotein A-V interaction with members of the low density lipoprotein receptor gene family. Biochemistry 2007;46:3896–3904. [PubMed: 17326667]

44. Beigneux AP, Davies BS, Gin P, Weinstein MM, Farber E, Qiao X, Peale F, Bunting S, Walzem RL, Wong JS, Blaner WS, Ding ZM, Melford K, Wongsiriroj N, Shu X, de Sauvage F, Ryan RO, Fong LG, Bensadoun A, Young SG. Glycosylphosphatidylinositol-anchored high-density lipoprotein-binding protein 1 plays a critical role in the lipolytic processing of chylomicrons. Cell. Metab 2007;5:279–291. [PubMed: 17403372]

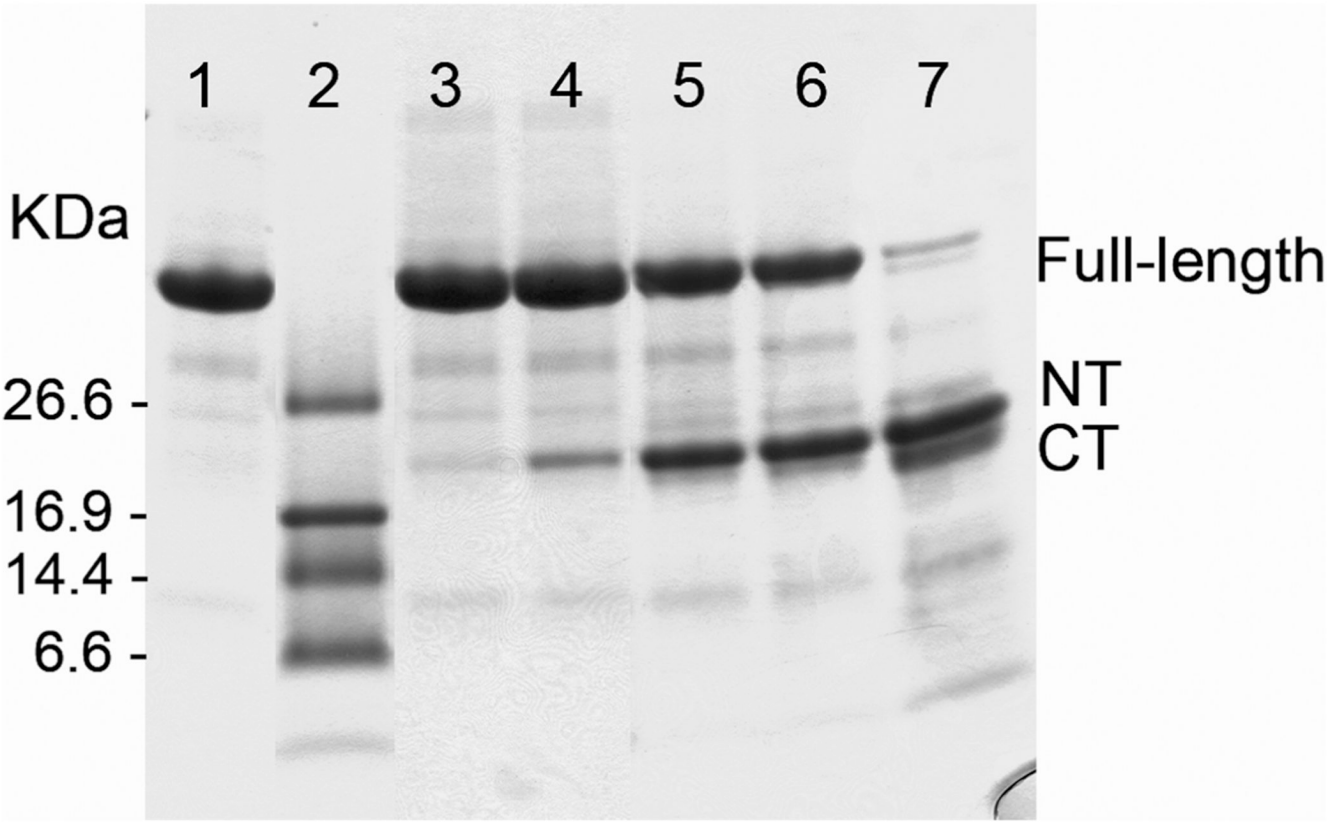

FIGURE 1.
SDS-PAGE analysis of pepsin-limited proteolysis of full-length apoA-V. Proteins were electrophoresed on a 10 to 20% acrylamide-SDS slab gel and stained with Gel Code Blue reagent: lane 1, untreated full-length apoA-V; lane 2, molecular mass markers; lane 3, pepsin-treated full-length apoA-V at 0 min; lane 4, pepsin treated for 5 min; lane 5, pepsin treated for 30 min; lane 6, pepsin treated for 60 min; and lane 7, pepsin treated for 120 min. NT denotes the N-terminal fragment and CT the C-terminal fragment.

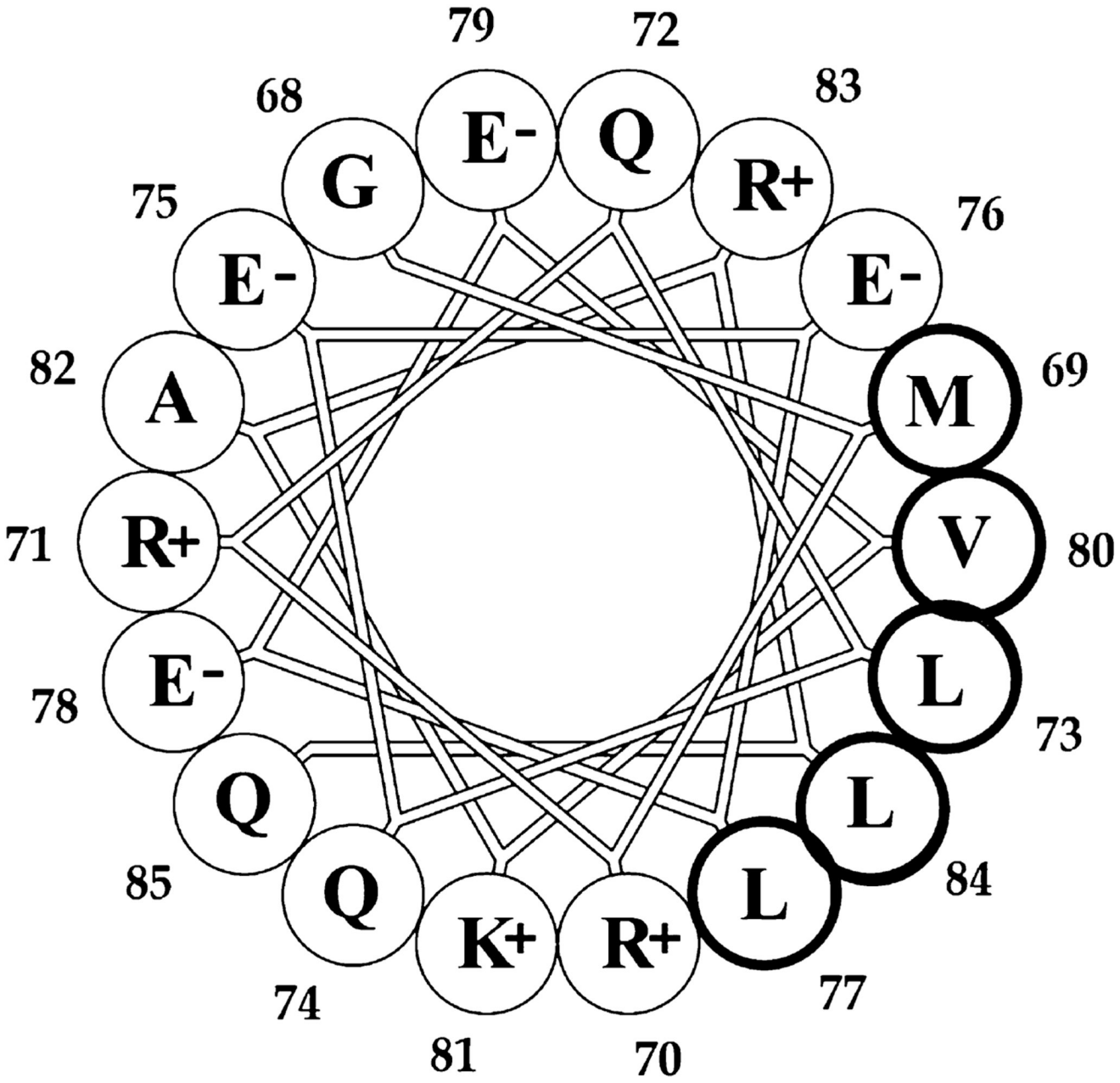

FIGURE 2.
Helical wheel diagram for a predicted helix in apoA-V(1–146). The amino acid residues depicted are numbered with hydrophobic residues circled in bold and charged residues indicated.

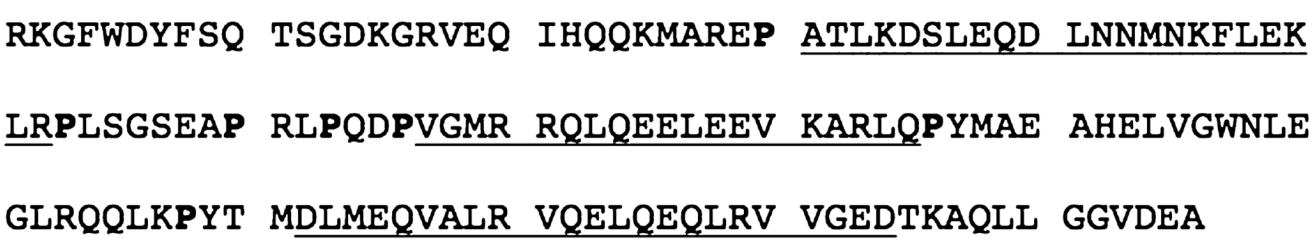

FIGURE 3.
Amino acid sequence of apoA-V(1–146). Residues postulated to adopt α-helical secondary structure, as predicted with Coils analysis, are underlined. Proline residues are depicted in bold.

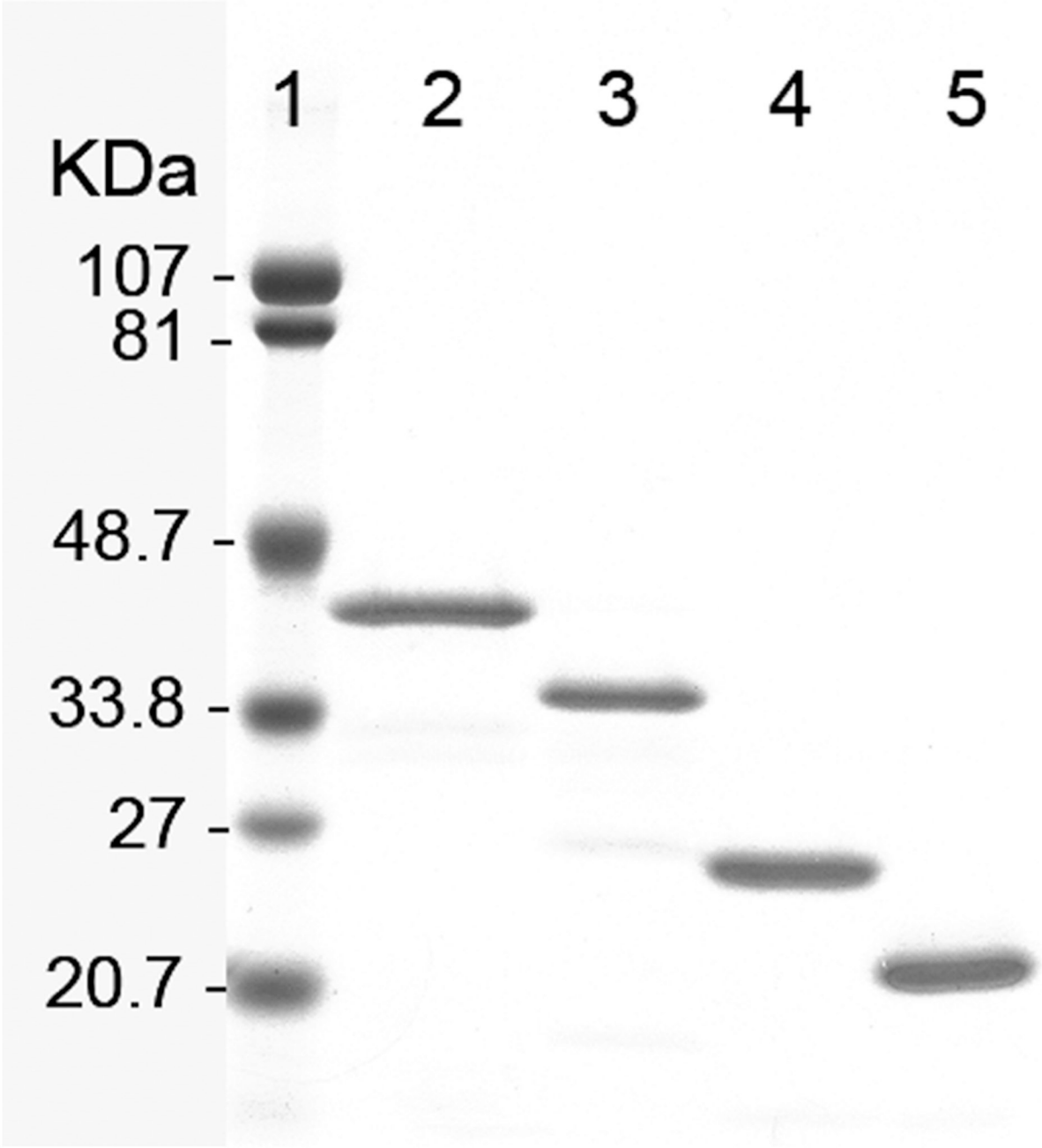

FIGURE 4.
SDS-PAGE analysis of isolated apoA-V truncation variants: lane 1, molecular mass markers; lane 2, full-length apoAV; lane 3, apoA-V(1–292); lane 4, apoA-V(1–169); and lane 5, apoA-V(1–146).

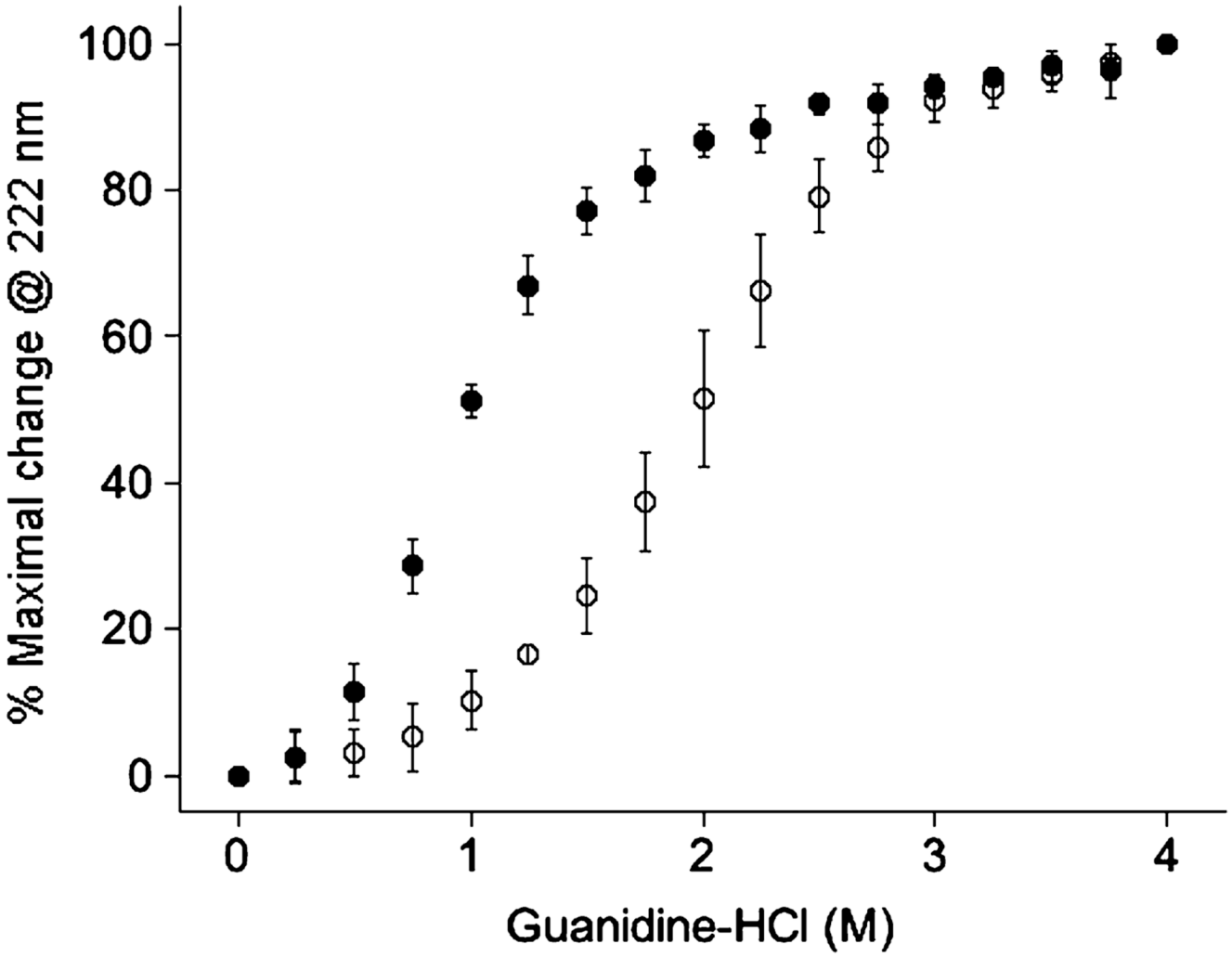

FIGURE 5.

Guanidine HCl denaturation of apoA-V(1–146). The molar ellipticity of the protein was measured at 222 nm at a concentration of 0.2 mg/mL in 50 mM citrate and 150 mM NaCl (pH 3.0) (○) or 20 mM phosphate buffer (pH 7.4) (●), at various concentrations of guanidine HCl (± standard deviation; $n = 4$).

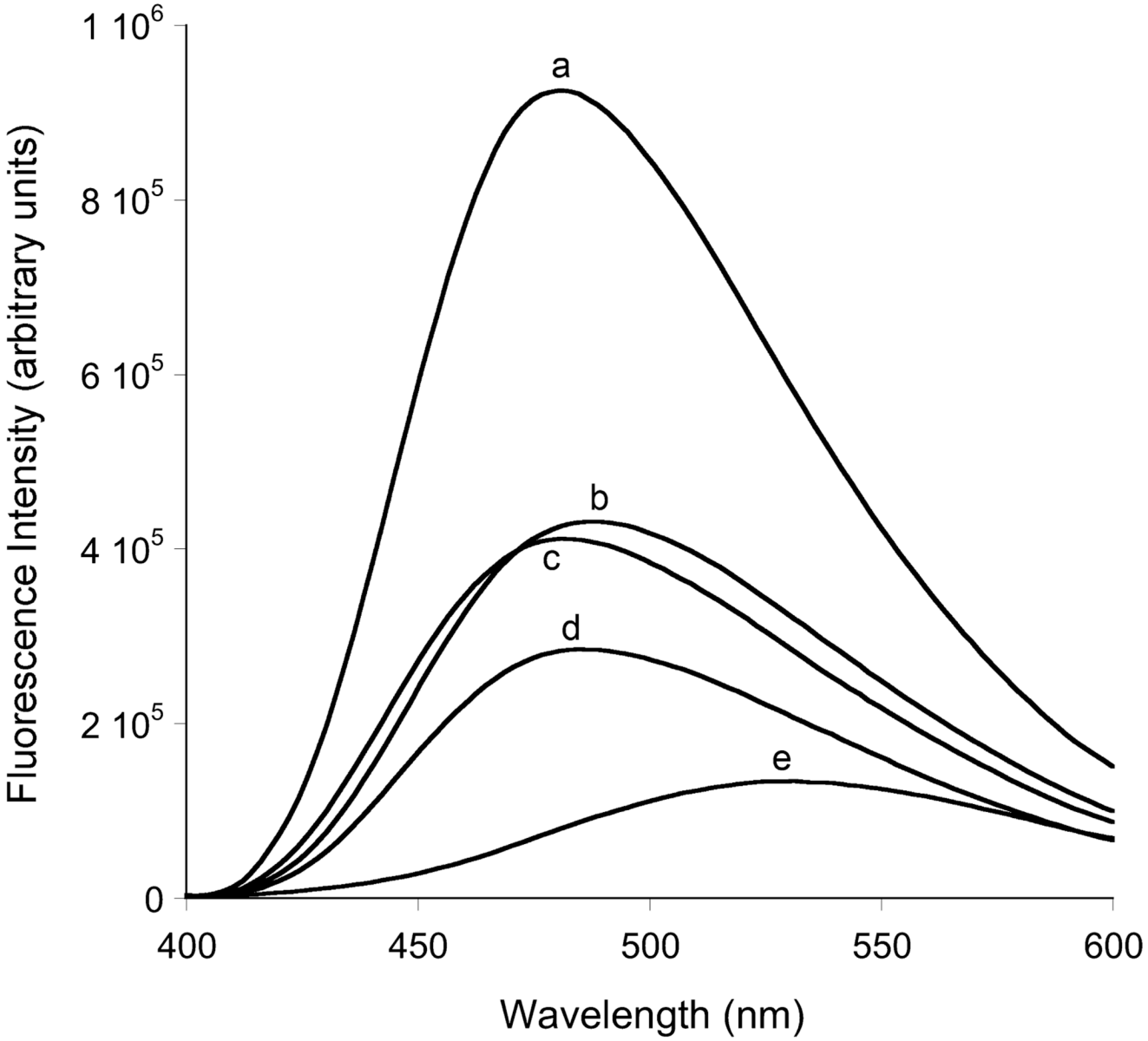

FIGURE 6.
Effect of proteins on ANS fluorescence: (a) albumin, (b) apoA-V(1–146), (c) apoLp III, (d) apoE3 NT, and (e) ANS in buffer.

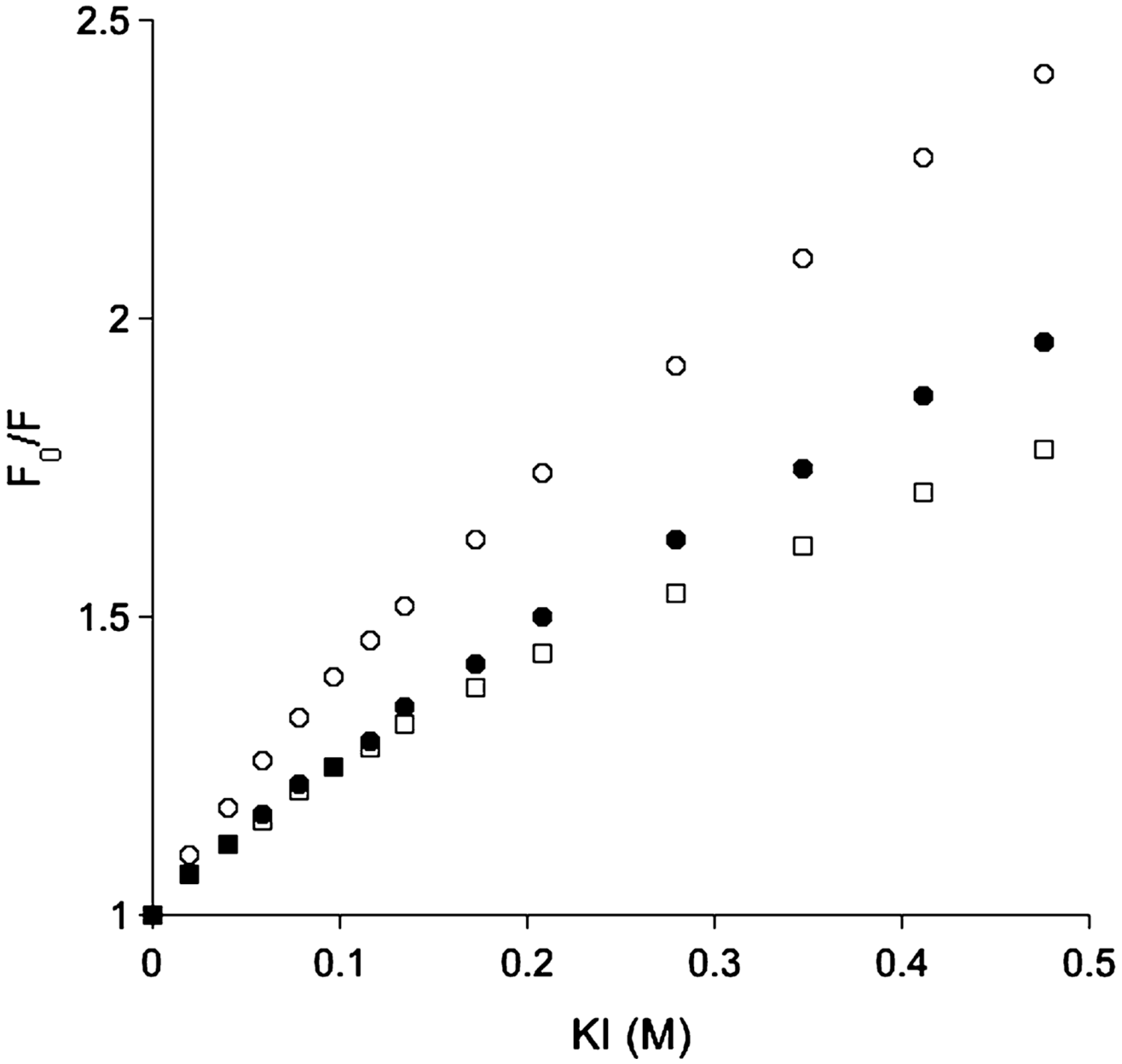

FIGURE 7.
Trp fluorescence quenching of apoA-V(1–146) by KI at pH 7.4. Stern–Volmer plots of apoA-V(1–146) Trp5 (○), apoA-V(1–146) Trp97 (●), and apoA-V(1–146) Trp73 (□).

Table 1

Result Summary of Sedimentation Velocity Runs on ApoA-V(1–146)

sample concentration (mg/mL)	$S_{20,w}$	$S°_{20,w}$	axial ratio
0.55	1.868	1.877	6.385
0.24	1.756	1.760	7.883

Table 2

Fluorescence Properties of ApoA-V(1–146) Single-Trp Variants[a]

	λ_{max} (nm)[b]	
	pH 7.4	**pH 3.0**
"wild type"	350	347
Trp5	349	348
Trp97	349	341
Trp73	349	338

[a] Spectra were recorded on a Horiba Jobin Yvon FluoroMax-4 luminescence spectrometer. Emission was scanned from 300 to 450 nm (excitation at 295 nm; 2.0 nm slit width for the excitation and emission monochromators). All spectra were recorded in either 20 mM sodium phosphate (pH 7.4) with 150 mM NaCl or 50 mM sodium citrate (pH 3.0) with 150 mM NaCl.

[b] λ_{max} is the wavelength of maximum fluorescence emission. Values are the means of three determinations. In all cases, the standard deviations were ≤1 nm.